

## **A SIMPLE DESIGN OF BROADBAND CROSS-POLARIZATION CONVERTER FOR THE THz FREQUENCY RANGE**

**Thi Minh Nguyen<sup>1,2,\*</sup>, Huu Lam Phan<sup>2</sup>, Hong Quang Nguyen<sup>2</sup>, Thanh Nghia Cao<sup>2</sup>,  
Ngoc Minh Luong<sup>2</sup>, Thi Kim Thu Nguyen<sup>2</sup>, Thi Minh Tam Nguyen<sup>2</sup>,  
Thi Huyen Thuong Ho<sup>2</sup>, Dinh Lam Vu<sup>1</sup>, Thi Quynh Hoa Nguyen<sup>2</sup>**

<sup>1</sup> Graduate University of Science and Technology,

Vietnam Academy of Science and Technology, HaNoi, Vietnam

<sup>2</sup> School of Engineering and Technology, Vinh university, NgheAn, Vietnam

### **ARTICLE INFORMATION ABSTRACT**

**Journal:** Vinh University  
Journal of Science  
ISSN: 1859-2228

**Volume:** 52  
**Issue:** 4A

**\*Correspondence:**  
minhntdhv@gmail.com

**Received:** 08 August 2023

**Accepted:** 19 September 2023

**Published:** 20 December 2023

#### **Citation:**

Thi Minh Nguyen, Huu Lam Phan, Hong Quang Nguyen, Thanh Nghia Cao, Ngoc Minh Luong, Thi Kim Thu Nguyen, Thi Minh Tam Nguyen, Thi Huyen Thuong Ho, Dinh Lam Vu, Thi Quynh Hoa Nguyen (2023). A simple design of broadband cross-polarization converter for the THz frequency range. *Vinh Uni. J. Sci.*

Vol. 52 (4A), pp. 28-38  
doi: 10.56824/vujs.2023a084

#### **OPEN ACCESS**

Copyright © 2023. This is an Open Access article distributed under the terms of the [Creative Commons Attribution License \(CC BY NC\)](#), which permits non-commercially to share (copy and redistribute the material in any medium) or adapt (remix, transform, and build upon the material), provided the original work is properly cited.

A broadband and lightweight polarization converter is proposed for applications in the THz frequency region. The proposed design has a metasurface structure with the dielectric layer modified to a hollow structure to obtain a lightweight design. The unit cell consists of two opposite arcs resonator patches and a continuous metal patch separated by the polyimide substrate layer. The simulated results indicate that the proposed polarized converter achieves a polarization conversion ratio above 93% in the frequency range from 1.6 THz to 5.8 THz with a relative bandwidth of 113.5%.

**Keywords:** Metasurfaces; broadband; cross polarization converter; THz frequency; lightweight.

### **1. Introduction**

In recent decades, Terahertz (THz) technology has evolved rapidly and gained popularity owing to its diversified potential applications in nondestructive testing, imaging, communications, and spectroscopy [1-4]. The manipulation of electromagnetic waves in this frequency range results in a variety of applications such as communication, astronomy, and medicine. One of the important properties of electromagnetic waves (EM) is their polarization state which specifies the direction of oscillation of their electric components. To highly effective control the polarization of the EM wave, the polarization converter is used [5-9]. Conventional polarization converters are currently constructed from natural materials such as quartz or liquid crystal with the birefringence effect. [10]. However, large sizes and thicknesses, narrow operating frequency bands, and incident angle responses are the drawbacks of these devices, making them inconsistent for many real-world applications. Consequently, various attempts have been undertaken to overcome the shortcomings of conventional

polarization converters [6, 11-20]. Among these methods, metamaterials (MMs), which are artificial metamaterials composed of sub-wavelength structure, are a new solution to miniaturize and expand the bandwidth of polarization converters [17, 18, 20].

Metasurface, as a sub-wavelength two-dimensional version of metamaterial, has the advantages of simple structure, low loss, and easy processing that can provide an effective strategy to manipulate the EM waves. Based on their prominent properties, several THz polarization converters using metasurfaces have been proposed successively for an efficient conversion. For example, Liu et al. recently proposed a linear reflective polarization converter using cross-shape metasurfaces that can operate in the frequency range of 0.8-1.6 THz [10]. Nevertheless, the polarization conversion ratio (PCR) and the relative bandwidth (RBW) of the proposed devices were quite low (85% and 75%, respectively) in the interesting band [10]. To enhance the polarization conversion efficiency, Ding et al. reported a THz broadband polarization converter based on circular-end graphene rectangles. The device could achieve an efficiency of over 94% from approximately 2.5 to 5 THz. However, the RBW was only 66% [21]. To improve the RBW of the polarization converter, Ako et al. demonstrated a broadband, wide-angle polarization converter through a T-shape metasurface with a RBW of 101.54% in the range of 0.34-1.04 THz. However, PCR was still low, less than 80% [22]. Therefore, designing a polarization converter to achieve both a simple, lightweight structure and a high conversion rate with a large RBW remains a major challenge.

In this paper, we propose a simple, lightweight structure, ultrawideband, and high-efficiency cross-polarization converter (CPC) using two opposite arc-shape metasurfaces. The proposed structure includes a metal resonator designed on a polyimide substrate and a metal ground layer deposited on another polyimide substrate, separated by an air gap. The air gap is used to achieve a lightweight structure with a wide bandwidth in a low working frequency range. The simulation results indicated that our polarization converter can operate in the frequency range from 1.6 to 5.8 THz with the RBW of 113.5%. In addition, the PCR efficiency of the proposed device exceeded 93% in the operating band. Moreover, its physical mechanism and insensitivity to the polarization angle were analyzed by simulation.

## 2. Designing and modeling

Fig. 1 shows a schematic of the proposed polarization converter. The structure consists of a periodic array of an anisotropic metasurface unit cell. The unit cell consists of two identical polyimide substrate layers separated from each other by an air gap, as shown in Fig. 1(a). The polyimide has a relative permittivity of 3.5 and a loss tangent of 0.0027. A metallic pattern designed on the upper polyimide substrate acts as a resonator. Meanwhile, another tal sheet backed the lower polyimide substrate serves as a ground plane. A gold sample with a thickness of 0.2  $\mu\text{m}$  ( $t$ ) is selected for the metal layer. The polarization converter is simulated using the commercial Computer Simulation Technology microwave studio 2015 software to optimize geometric parameters. The detailed geometric parameters of the unit-cell structure are shown in Fig. 1(b)-(c), in which  $P = 40 \mu\text{m}$ ,  $R = 19 \mu\text{m}$ ,  $r = 15.6 \mu\text{m}$ ,  $h_s = 0.8 \mu\text{m}$ ,  $h_a = 18.2 \mu\text{m}$ ,  $m = 14 \mu\text{m}$ .

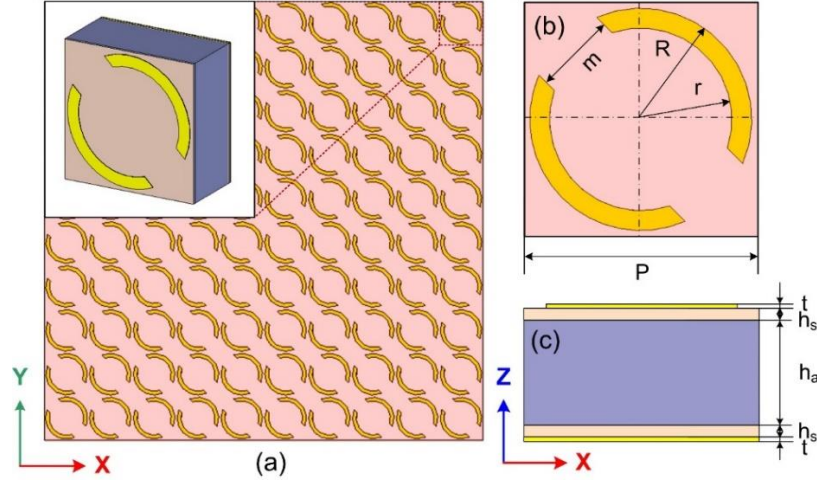


**Fig. 1:** Schematic of the proposed polarization converter  
(a) 3D view (b) top-view and (c) side-view

The boundary conditions of the unit cell are applied to the  $x$ - and  $y$ -directions, while the open conditions are fixed to the  $z$ -direction. The unit cell is symmetrical along the diagonal directions, the outcomes of  $y$ -polarized incidence are analogous to those of  $x$ -polarized incidence at normal incident waves. Therefore, the  $y$ -polarized incidence is used to analyze in simulation. In addition, the reflected EM-wave comprises both cross- and co-polarized components. The cross-polarized reflection coefficient  $r_{xy}$  and the co-polarized reflection coefficient  $r_{yy}$  are defined by eq. (1) and eq. (2), respectively [23].

$$r_{xy} = \frac{|E_{xr}|}{|E_{yi}|}, \quad (1)$$

$$r_{yy} = \frac{|E_{yr}|}{|E_{yi}|}. \quad (2)$$

and the performance of polarization converters is evaluated by the PCR given by

$$PCR = \frac{|r_{xy}|^2}{|r_{xy}|^2 + |r_{yy}|^2} \quad (3)$$

### 3. Results and discussion

Fig. 2(a) shows the simulated amplitude of co- and cross-polarization coefficients of the converter under transverse electric (TE) mode. It indicates that the four resonant peaks are indexed at 1.74 THz, 3.13 THz, 5.1 THz, and 5.7 THz. At these peaks, the amplitudes of co-reflection coefficients are 0.014, 0.005, 0.012, and 0.052 and the amplitudes of cross-reflection coefficients are 0.982, 0.987, 0.969, and 0.914, respectively. In addition, the cross-polarization is greater than 0.900 and the co-polarization factor is less than 0.203 in the frequency range from 1.6 THz to 5.8 THz. Fig. 2(b) shows that the PCR is close to 100% at the resonant frequencies. Furthermore, the PCR is higher than 93% in the range from 1.6 THz to 5.8 THz with a RBW of 113.5%. Therefore, the proposed CPC can effectively work as an ultra-broadband cross-polarization converter. The different phase of the co- and the cross-polarization coefficient is illustrated in Fig. 2(b). The phase difference ( $\Delta_j$ ) is  $\pm 90^\circ$  in the whole operation band.

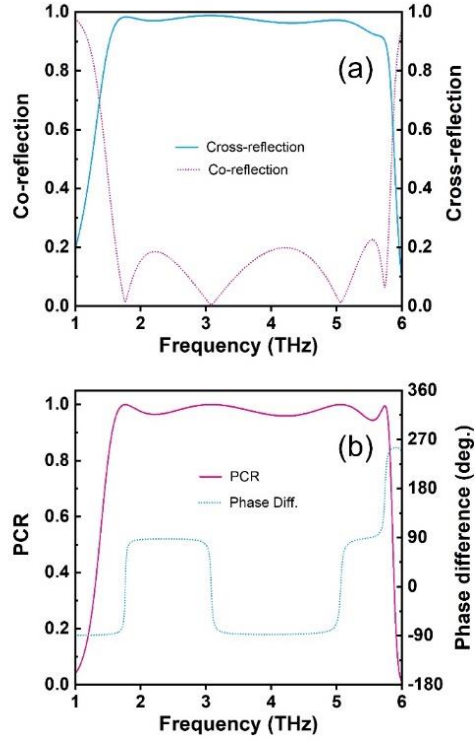


**Fig. 2:** (a) Simulated magnitude of co- and cross-polarization reflections and (b) Simulated PCR versus frequency under normal incidence and TE mode and phase difference of cross- and co-polarized reflection coefficients of the proposed converter

The working principle of the CPC is presented in Fig. 3. The y-polarized incident EM wave ( $E_i$ ) can decompose into u- and v-components. The u- and v-axes are rotated  $\pm 45^\circ$  to the y-axis, as shown in Fig. 3. The incident and reflection waves are given by eq. (4) and eq. (5) respectively [24].

$$E_i = \hat{y}E_y = \hat{u}E_{iu} + \hat{v}E_{iv} \quad (4)$$

$$E_r = \hat{u}E_{ru} + \hat{v}E_{rv} \\ = \hat{u}(r_{uu}E_{iu}e^{i\Phi_{uu}} + r_{uv}E_{iv}e^{i\Phi_{uv}}) + \hat{v}(r_{vv}E_{iv}e^{i\Phi_{vv}} + r_{vu}E_{iu}e^{i\Phi_{vu}}) \quad (5)$$

where,  $\hat{u}$  and  $\hat{v}$  are the unit vectors;  $r_{uu}$ ,  $\Phi_{uu}$  and  $r_{vv}$ ,  $\Phi_{vv}$  are amplitude and phase of co-reflection coefficients for u-to-u and v-to-v polarization conversion, respectively;  $r_{vu}$ ,  $\Phi_{vu}$  and  $r_{uv}$ ,  $\Phi_{uv}$  are amplitude and phase of cross reflection coefficients for u-to-v and v-to-u polarization conversion, respectively. The proposed converter yields anisotropic properties with dispersive relative permittivity and permeability because of its asymmetric structure. Thus, there is a difference in the phase and amplitude of reflection waves in the u- and v-components.

If

$$r_{uu} = r_{vv} \approx 1, r_{uv} = r_{vu} \approx 0, \text{ and} \\ \Delta_\varphi = \Phi_{uu} - \Phi_{vv} = 180^\circ + 2k\pi \text{ (k is an integer),}$$

the synthetic fields of  $E_{ru}$  and  $E_{rv}$  will lie along the x-axis. It means that the polarized incident wave is rotated  $90^\circ$  and the converter reveals a cross-polarization conversion.

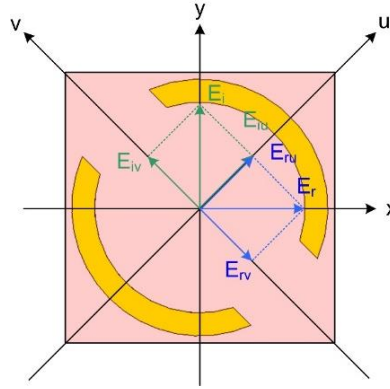


**Fig. 3:** *The working principle of the proposed polarization converter*

Fig. 4 shows the amplitude of reflection coefficients and phase difference for the  $u$ - and  $v$ -components. From Fig. 4(a), the amplitudes of the co- and cross-polarized reflection coefficients are nearly equal to 1 and 0 for the entire survey frequency range of 1.6–5.8 THz, respectively. Furthermore, the phase difference between the  $u$ - and  $v$ -components is approximately  $180^\circ \pm 23^\circ$  in the range of 1.6–5.8 THz. Furthermore, at the four resonant points 1.74 THz, 3.13 THz, 5.1 THz, and 5.7 THz, the phase difference between the  $u$ - and  $v$ -components is  $180^\circ$ .

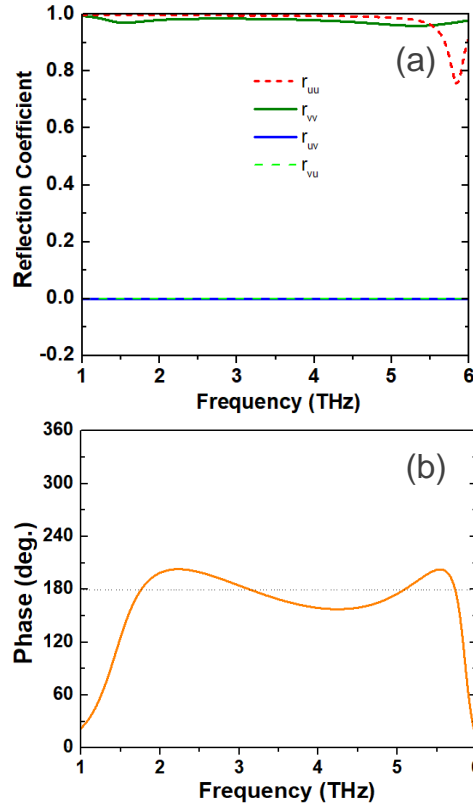


**Fig. 4:** (a) Amplitude and (b) phase difference of the reflection coefficients of the proposed converter for  $u$ - and  $v$ -components at the normal incidence

To better understand the physical mechanism of the proposed PC, the distributions of the electric field and the surface current on the front and back metasurface structures are investigated at four resonant frequencies: 1.74 THz, 3.13 THz, 5.1 THz, and 5.7 THz, as shown in Fig. 5. It is shown that the electric fields are accumulated in some specific regions of the CPC structure at a specified frequency. The electric field is formed at the edge and the outer face of the metal resonator.

In Figs. 5, the direction of the arrows represents the direction of the surface current distribution at the four resonant frequencies. As shown in Fig. 5(e), 5(i), Fig. 5(f), (j), and Fig. 5(h), 5(l), the surface currents on the top layer are parallel and opposite to the underlayer metal floor currents at 1.74 THz, 3.13 THz, and 5.7 THz, respectively. It implies that these resonant frequencies are influenced by magnetic resonance [25-27]. In contrast, at a frequency of 5.1 THz, the surface current on the top layer is parallel and in the same direction to the underlayer metal floor current, which is provided by electric resonance [25-27]. These multiple resonances play a vital role to obtain the high polarization conversion efficiency in a wide band for the proposed polarization converter.

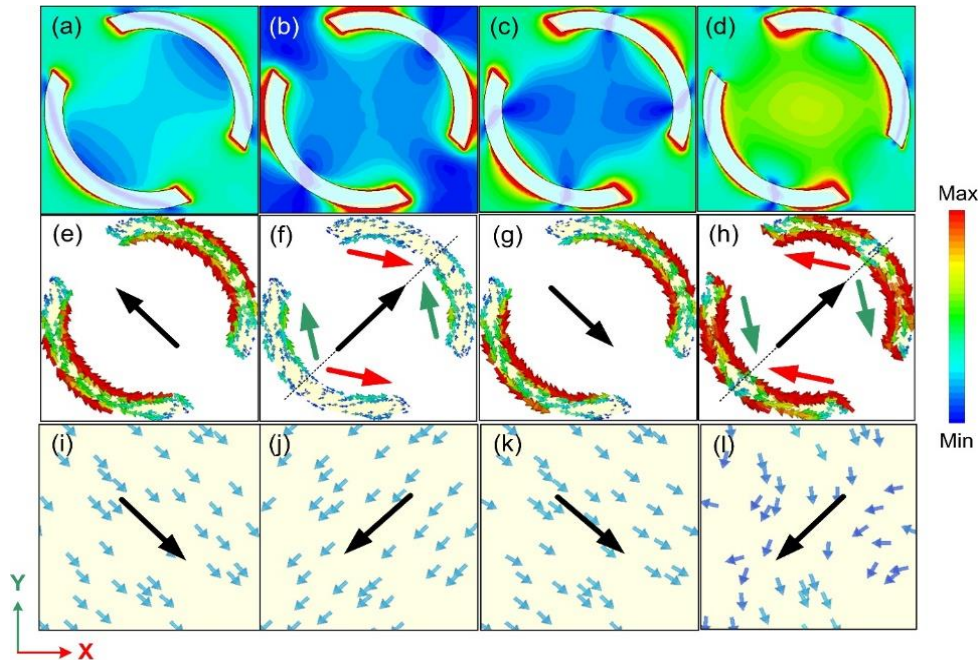


**Fig. 5:** The simulated results for (a), (b), (c), and (d) electric field of the proposed converter at the resonant frequencies; Surface current distributions on the (e)-(h) top layers and (i)-(l) metallic ground sheet of the polarization converter unit cell at the four resonant frequencies

In addition, the effect of geometrical parameters on the performance of the proposed polarization converter is analyzed. The PCR of the proposed converter is simulated at different values of  $P$ ,  $m$ ,  $R$ , and  $r$ . The results of the survey of the parameters of the structure are depicted in Fig 6. To achieve the highest polarization conversion and widest bandwidth,  $P$ ,  $m$ ,  $R$ , and  $r$  are optimized at 40  $\mu\text{m}$ , 19  $\mu\text{m}$ , 15.6  $\mu\text{m}$ , and 14  $\mu\text{m}$  respectively.

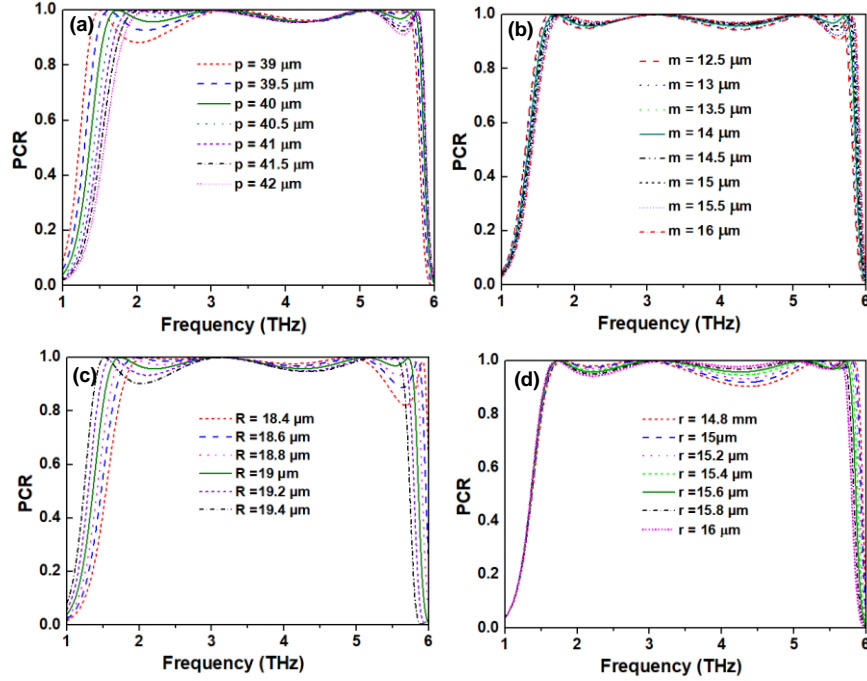


**Fig. 6:** The PCR with various unit cell parameters of the proposed polarization converter: (a)  $P$ , (b)  $m$ , (c)  $R$ , and (d)  $r$

Furthermore, the dependence of the PCR on the incident angles is investigated in the range of  $0^\circ$ -  $50^\circ$  for both transverse electric (TE) and transverse magnetic (TM) polarizations, as depicted in Fig. 7(a) and 7(b), respectively. As the incident angle increases, the bandwidth of the proposed polarization converter is reduced for both polarizations. This phenomenon could be caused by the destructive interference at the surface of the metasurface structure with large incident angles. However, the PCR is maintained above 93% when the incident angle changes from  $0^\circ$  to  $10^\circ$  in the whole band from 1.6 THz to 5.8 THz. In addition, the PCR remains above 80% when the incident angle is less than  $30^\circ$ . It is worth noting that the PCR decreases rapidly at around 3.5 THz for both TE and TM modes, which is attributed to the strong absorption at that frequency. However, our design still has a high polarization conversion efficiency when the incident angle changes from  $0^\circ$  to  $30^\circ$  in these bands from 1.6 THz to 3.5 THz and 3.5 THz to 4.7 THz.

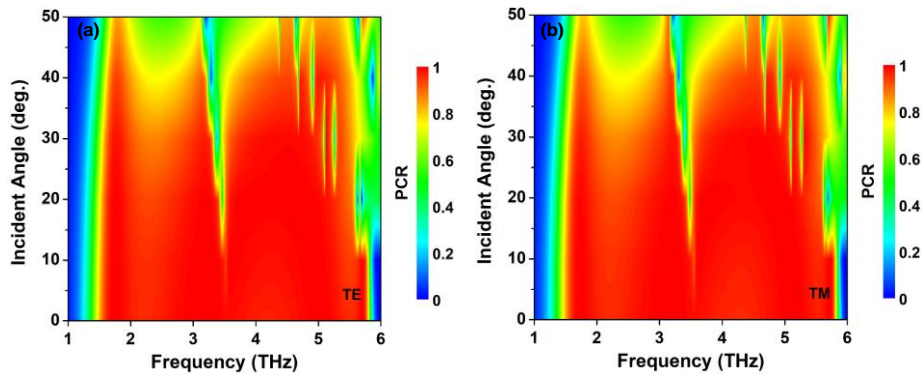


**Fig. 7:** Simulated PCR versus frequency of the polarization conversion as a function of the incident angle (a) TE and (b) TM modes

Table 1 is the performance comparison of the proposed polarization converter with previous polarization converters. It shows that the proposed converter has excellent performance and wide bandwidth.

**Table 1:** Performance comparison of the proposed polarization converter with previous polarization converters

Ref	Working Frequency (THz) with PCR $\geq$ 85%	RBW (%)	Incident angle insensitivity (PCR above 80%)
[28]	3.75 – 11.35	100,6	20
[10]	1.07 – 1.35	39	None
[29]	4.86 – 8.42	54	25
[30]	2 – 2.6	26.1	30
<b>This work</b>	1.55 – 5.82	113.5%.	30

#### 4. Conclusion

A wideband cross-polarization converter based on metasurface has been presented. The results show that the proposed polarization converter converts linear-polarized incident EM waves into their cross-polarized reflective counterparts with high polarization conversion efficiency above 93% in an ultrawide frequency range from 1.6 THz to 5.8 THz. This operating frequency band corresponds to an RBW of 113.5%. Besides, the proposed structure exhibits fairly good angular stability in the polarization conversion operation. Table 1 shows the performance comparison of the proposed polarization converter with some reported polarization converters. Due to the excellent performance of the proposed architecture, it has great application for devices working in the terahertz region.

#### Acknowledgments

This work is supported by the Ministry of Education and Training, Vietnam (Grant Number B2022-TDV-04).

#### REFERENCES

- [1] K. Nicholas, Z. Hua, X. Jingzhou, I. L. Kuang, H. Jenn-Shyong, and Z. Xi-Cheng, "Non-destructive sub-THz CW imaging," in *Proc.SPIE*, vol. 5727, pp. 132-142, 2005.
- [2] Z. D. Taylor *et al.*, "THz Medical Imaging: in vivo Hydration Sensing," *IEEE Transactions on Terahertz Science and Technology*, vol. 1, no. 1, pp. 201-219, 2011. DOI: [10.1109/TTHZ.2011.2159551](https://doi.org/10.1109/TTHZ.2011.2159551)
- [3] J. F. Federici *et al.*, "THz imaging and sensing for security applications-explosives, weapons and drugs," *Semiconductor Science and Technology*, vol. 20, no. 7, p. S266, 2005. DOI: [10.1088/0268-1242/20/7/018](https://doi.org/10.1088/0268-1242/20/7/018)
- [4] H. B. Liu, H. Zhong, N. Karpowicz, Y. Chen, and X. C. Zhang, "Terahertz Spectroscopy and Imaging for Defense and Security Applications," *Proceedings of*

- the IEEE*, vol. 95, no. 8, pp. 1514-1527, 2007. DOI: [10.1109/JPROC.2007.898903](https://doi.org/10.1109/JPROC.2007.898903)
- [5] M. Feng, J. Wang, H. Ma, W. Mo, H. Ye, and S. Qu, "Broadband polarization rotator based on multi-order plasmon resonances and high impedance surfaces," *Journal of Applied Physics*, vol. 114, no. 7, p. 074508, 2013. DOI: [10.1063/1.4819017](https://doi.org/10.1063/1.4819017)
- [6] H. Chen *et al.*, "Ultra-wideband polarization conversion metasurfaces based on multiple plasmon resonances," *Journal of Applied Physics*, vol. 115, no. 15, p. 154504, 2014. DOI: [10.1063/1.4869917](https://doi.org/10.1063/1.4869917)
- [7] L. Cong *et al.*, "A perfect metamaterial polarization rotator," *Applied Physics Letters*, vol. 103, no. 17, p. 171107, 2013. DOI: [10.1063/1.4826536](https://doi.org/10.1063/1.4826536)
- [8] T. K. T. Nguyen *et al.*, "Simple design of efficient broadband multifunctional polarization converter for X-band applications," *Scientific Reports*, vol. 11, no. 1, p. 2032, 2021. DOI: [10.1038/s41598-021-81586-w](https://doi.org/10.1038/s41598-021-81586-w)
- [9] C.-p. Huang, Q.-j. Wang, X.-g. Yin, Y. Zhang, J.-q. Li, and Y.-y. Zhu, "Break Through the Limitation of Malus' Law with Plasmonic Polarizers," *Advanced Optical Materials*, vol. 2, no. 8, pp. 723-728, 2014. DOI: [10.1002/adom.201400111](https://doi.org/10.1002/adom.201400111)
- [10] W. Liu *et al.*, "Ultra-efficiency broadband terahertz polarization converter based on a cross-shaped metamaterial," *AIP Advances*, vol. 12, no. 8, p. 085101, 2022. DOI: [10.1063/5.0098815](https://doi.org/10.1063/5.0098815)
- [11] W. Mo, X. Wei, K. Wang, Y. Li, and J. Liu, "Ultrathin flexible terahertz polarization converter based on metasurfaces," *Optics Express*, vol. 24, no. 12, pp. 13621-13627, 2016. DOI: [10.1364/OE.24.013621](https://doi.org/10.1364/OE.24.013621)
- [12] L. Dai, Y. Zhang, H. Zhang, and J. J. A. P. E. F. O'Hara, "Broadband tunable terahertz cross-polarization converter based on Dirac semimetals," vol. 12, 2019. DOI: [10.7567/1882-0786/ab25c4](https://doi.org/10.7567/1882-0786/ab25c4)
- [13] A. K. Fahad *et al.*, "Ultra-Thin Metasheet for Dual-Wide-Band Linear to Circular Polarization Conversion With Wide-Angle Performance," *IEEE Access*, vol. 8, pp. 163244-163254, 2020. DOI: [10.1109/ACCESS.2020.3021425](https://doi.org/10.1109/ACCESS.2020.3021425)
- [14] X. Huang, H. Yang, D. Zhang, and Y. Luo, "Ultrathin Dual-Band Metasurface Polarization Converter," *IEEE Transactions on Antennas and Propagation*, vol. 67, no. 7, pp. 4636-4641, 2019. DOI: [10.1109/TAP.2019.2911377](https://doi.org/10.1109/TAP.2019.2911377)
- [15] P. Xu, S.-Y. Wang, and W. Geyi, "A linear polarization converter with near unity efficiency in microwave regime," *Journal of Applied Physics*, vol. 121, no. 14, p. 144502, 2017. DOI: [10.1063/1.4979880](https://doi.org/10.1063/1.4979880)
- [16] T. Q. H. Nguyen *et al.*, "Simple design of a wideband and wide-angle reflective linear polarization converter based on crescent-shaped metamaterial for Ku-band applications," *Optics Communications*, vol. 486, p. 126773, 2021. DOI: [10.1016/j.optcom.2021.126773](https://doi.org/10.1016/j.optcom.2021.126773)
- [17] Z. Zhang *et al.*, "Single-layer metasurface for ultra-wideband polarization conversion: bandwidth extension via Fano resonance," *Scientific Reports*, vol. 11, no. 1, p. 585, 2021. DOI: [10.1038/s41598-020-79945-0](https://doi.org/10.1038/s41598-020-79945-0)
- [18] F. Zhang, G. M. Yang, and Y. Q. Jin, "Microwave Polarization Converter with Multilayer Metasurface," in *2020 14th European Conference on Antennas and*

- Propagation (EuCAP)*, pp. 1-4, 2020. DOI: [10.23919/EuCAP48036.2020.9135879](https://doi.org/10.23919/EuCAP48036.2020.9135879)
- [19] L. S. Ren, Y. C. Jiao, F. Li, J. J. Zhao, and G. Zhao, "A Dual-Layer T-Shaped Element for Broadband Circularly Polarized Reflectarray With Linearly Polarized Feed," *IEEE Antennas and Wireless Propagation Letters*, vol. 10, pp. 407-410, 2011. DOI: [10.1109/LAWP.2011.2148090](https://doi.org/10.1109/LAWP.2011.2148090)
- [20] C. Fu, Z. Sun, L. Han, C. Liu, T. Sun, and P. K. Chu, "High-Efficiency Dual-Frequency Reflective Linear Polarization Converter Based on Metasurface for Microwave Bands," *Applied Sciences*, vol. 9, no. 9, 2019. DOI: [10.3390/app9091910](https://doi.org/10.3390/app9091910)
- [21] Y. Ding, Y. Chang, and J. Yao, "Ultrabroad reflective polarization converter in terahertz based on circular-end graphene rectangles," *Europhysics Letters*, vol. 140, no. 6, p. 65001, 2022. DOI: [10.1209/0295-5075/aca353](https://doi.org/10.1209/0295-5075/aca353)
- [22] R. T. Ako, W. S. L. Lee, M. Bhaskaran, S. Sriram, and W. Withayachumnankul, "Broadband and wide-angle reflective linear polarization converter for terahertz waves," *APL Photonics*, vol. 4, no. 9, p. 096104, 2019. DOI: [10.1063/1.5116149](https://doi.org/10.1063/1.5116149)
- [23] Deng, G.; Sun, H.; Lv, K.; Yang, J.; Yin, Z.; Chi, B. An efficient wideband cross-polarization converter manufactured by stacking metal/dielectric multilayers via 3D printing. *J. Appl. Phys.*, 127, 093103, 2020. DOI: [10.1063/1.5135632](https://doi.org/10.1063/1.5135632)
- [24] M. I. Khan, Z. Khalid, and F. A. Tahir, "Linear and circular-polarization conversion in X-band using anisotropic metasurface," *Scientific Reports*, vol. 9, no. 1, p. 4552, 2019. DOI: [10.1038/s41598-019-40793-2](https://doi.org/10.1038/s41598-019-40793-2)
- [25] Y. Qi, B. Zhang, C. Liu, and X. Deng, "Ultra-Broadband Polarization Conversion Meta-Surface and its Application in Polarization Converter and RCS Reduction," *IEEE Access*, vol. 8, pp. 116675-116684, 2020. DOI: [10.1109/ACCESS.2020.3004127](https://doi.org/10.1109/ACCESS.2020.3004127)
- [26] T. N. Cao, M. T. Nguyen, N. Hieu Nguyen, C. L. Truong, and T. Q. H. Nguyen, "Numerical design of a high efficiency and ultra-broadband terahertz cross-polarization converter," *Materials Research Express*, vol. 8, no. 6, p. 065801, 2021. DOI: [10.1088/2053-1591/ac0369](https://doi.org/10.1088/2053-1591/ac0369)
- [27] J. Xu, R. Li, J. Qin, S. Wang, and T. Han, "Ultra-broadband wide-angle linear polarization converter based on H-shaped metasurface," *Optics Express*, vol. 26, no. 16, pp. 20913-20919, 2018. DOI: [10.1364/OE.26.020913](https://doi.org/10.1364/OE.26.020913)
- [28] M. Sajjad, X. Kong, S. Liu, A. Ahmed, S. Ur Rahman, and Q. Wang, "Graphene-based THz tunable ultra-wideband polarization converter," *Physics Letters A*, vol. 384, no. 23, p. 126567, 2020. DOI: [10.1016/j.physleta.2020.126567](https://doi.org/10.1016/j.physleta.2020.126567)
- [29] R. Sarkar, A. Bhattacharya, A. Punjal, S. Prabhu, and G. Kumar, "Broadband terahertz polarization conversion using a planar toroidal metamaterial," *Journal of Applied Physics*, vol. 132, p. 183103, 2022. DOI: [10.1063/5.0112004](https://doi.org/10.1063/5.0112004)
- [30] D. Yu *et al.*, "Photo-Excited Switchable Terahertz Metamaterial Polarization Converter/Absorber," *Crystals*, vol. 11, no. 9, 2021. DOI: [10.3390/cryst11091116](https://doi.org/10.3390/cryst11091116)

## TÓM TẮT

### THIẾT KẾ VẬT LIỆU BIẾN HOÁ PHÂN CỰC CHÉO BẰNG THÔNG RỘNG LÀM VIỆC TRONG VÙNG TẦN SỐ THz

Nguyễn Thị Minh<sup>1,2</sup>, Phan Hữu Lâm<sup>2</sup>, Nguyễn Hồng Quảng<sup>2</sup>,  
Cao Thành Nghĩa<sup>2</sup>, Lương Ngọc Minh<sup>2</sup>, Nguyễn Thị Kim Thu<sup>2</sup>,  
Nguyễn Thị Minh Tâm<sup>2</sup>, Hồ Thị Huyền Thương<sup>2</sup>,  
Vũ Đình Lâm<sup>1</sup>, Nguyễn Thị Quỳnh Hoa<sup>2</sup>

<sup>1</sup> Viện Hàn lâm khoa học và Công nghệ Việt Nam, Hà Nội, Việt Nam

<sup>2</sup> Viện Kỹ thuật và công nghệ, Trường Đại học Vinh, Nghệ An, Việt Nam

Ngày nhận bài 08/8/2023, ngày nhận đăng 19/9/2023

Bộ chuyển đổi phân cực sóng điện từ băng thông rộng dựa trên siêu vật liệu (hay vật liệu biến hóa) có trọng lượng nhẹ được đề xuất cho các ứng dụng trong vùng tần số Terahertz. Siêu vật liệu đề xuất có cấu trúc siêu bề mặt với lớp điện môi được điều chỉnh thành cấu trúc rỗng để giảm thiểu trọng lượng. Cấu trúc ô đơn vị gồm hai cung tròn bằng kim loại đối xứng nhau ở lớp trên cùng và một bản kim loại ở lớp dưới, ngăn cách nhau bởi các lớp chất nền polyimide. Kết quả mô phỏng cho thấy siêu vật liệu chuyển đổi phân cực đề xuất đạt tỷ lệ chuyển đổi phân cực trên 93% trong dải tần từ 1.6 THz đến 5.8 THz với băng thông tương đối là 113.5%.

**Từ khóa:** Siêu bề mặt; băng thông rộng; siêu vật liệu chuyển đổi phân cực; dải tần THz; trọng lượng nhẹ.